Effect of Carboxy-Functionalized Multiwall Nanotubes (MWNT−COOH) on the Crystallization and Chain Conformations of Poly(ethylene terephthalate) PET in PET−MWNT Nanocomposites

Spiros Tzavalas,[†] Vasilis Drakonakis,[†] Dionysis E. Mouzakis,[‡] Dieter Fischer,[§] and Vasilis G. Gregoriou*,[†]

Foundation for Research and Technology−Hellas, Institute of Chemical Engineering and High-Temperature Chemical Processes (FORTH/ICE-HT), Patras 26504, Greece, Department of Material Science, University of Patras, Patras, Greece, and Leibniz Institute of Polymer Research Dresden (IPF), D-01069 Dresden, Germany

Received June 19, 2006; Revised Manuscript Received October 11, 2006

ABSTRACT: Multiwall nanotubes that have undergone acidic treatment of varying duration were melt-compounded with poly(ethylene terephthalate) (PET) in a batch-mixer in order to create nanocomposite structures. The samples were pressed into films and annealed above the crystallization temperature of the polymer. Fourier Transform infrared (FT-IR) as well as Raman spectroscopies were utilized to monitor the gauche to trans transformations due to the annealing process with respect to the duration of the treatment of nanotubes. In addition, differential scanning calorimetry (DSC) measurements were performed to study the crystallinity changes due to the presence of the tubes. Acid-treated nanotubes were found not only to increase PET's crystallinity but also lead to a much better crystalline formation of the polymeric chains. The spectroscopic measurements in correlation with the DSC findings showed that neat PET has relatively more trans conformers in the noncrystalline phase than the PET−MWNT nanocomposite samples. Therefore, the presence of the nanotubes transforms the trans conformers of the noncrystalline phase into crystalline domains with the nanotubes acting as moderate nucleation agents.

Introduction

Carbon nanotubes (CNTs) have attracted much attention due to their superior mechanical, thermal and electrical properties,[1] since their discovery by Iijima (1991).[2] In particular they possess elastic modulus up to 1 TPa, thermal conductivity twice as high as that of diamond and electric current-carrying ability 1000 times that of copper wires.[3] Their unique properties led to innumerable potential applications for these materials such as in: field emitting diodes (FEDs),[4−6] emitting field effect transistors,[7] scanning microscopy,[8,9] lithium batteries,[10] hydrogen storage,[11−13] single electron transistors,[14] gas sensors,[15,16] composite materials, etc.

Poly(ethylene terephthalate) (PET) is of major industrial importance due to its low cost and high performance (since it has high glass transition and melting temperatures) as well as good physical properties. It has found a variety of applications such as in textile fibers, films, bottles containers, food packaging materials, engineering plastics in automobiles, electronics, etc. Its properties depend mainly on the degree of orientation of the polymer chains as well as the level of crystallinity.

Crystalline PET consists of fully trans conformers.[23−26] In particular, the ethylene glycol segment through rotation around the C−C bond adopts the trans (T) conformation, as well as the glycol group with respect to the C−O bond which is in trans (t) form. Additionally, the two carbonyl groups in each benzene ring are trans (T_B) with respect to each other.[24] Nevertheless it has been reported that the true crystalline structure contains also folded chains involving gauche conformers.[27] The case is not that clear though when it comes to amorphous PET. Even if amorphous PET is considered to bear mainly gauche conformers (10% trans)[28−30] several authors have reported noncrystalline PET consisting of mainly trans conformers.[31,32] In most cases though, two structures seem to coexist within the amorphous part of a PET sample; a completely disordered amorphous structure and an "intermediate" amorphous structure.[33] Thus, PET would be better described by a three phase model comprising: (a) a crystalline phase constituted exclusively of trans conformers, (b) an "intermediate" phase constituted of trans conformers that do not belong to crystalline phase, and (c) a third phase, which is completely disordered and contains mainly gauche conformers.[34]

PET−nanotube composites have been studied recently for their possible application in fuel cells,[17,18] flexible vapor sensors,[19] conductive fibers,[20] and composite materials with functionalized[21] and acid-treated[22] nanotubes. The main aim of the present work was to study the effect that the addition of nanotubes bears on the crystallization behavior, crystallinity, and chain conformations of poly(ethylene terephthalate). For this purpose acid-treated nanotubes were melt-mixed with poly(ethylene terephthalate) yielding PET−MWNT nanocomposites. The samples were subsequently annealed to assist the crystallization of the polymer. This is the first time, to our knowledge, that the trans and gauche conformations of the polymeric chains of PET were studied in the presence of nanotubes showing that the addition of the nanotubes alters the relative distribution of these units in the polymeric chains thus affecting its final crystallinity content. The acidic treatment was utilized to introduce carboxy groups onto the surface of carbon nanotubes so as to increase their chemical affinity with PET and also to reduce the $\pi-\pi$ stacking effect among the aromatic rings of

* To whom correspondence should be addressed. E-mail: gregoriou@iceht.forth.gr. Telephone: 0030-2610-965205. Fax: 0030-2610-965223.
[†] Foundation for Research and Technology−Hellas, Institute of Chemical Engineering and High-Temperature Chemical Processes (FORTH/ICE-HT).
[‡] Department of Material Science, University of Patras.
[§] Leibniz Institute of Polymer Research Dresden (IPF).

10.1021/ma0613584 CCC: $33.50
Published on Web 11/18/2006

Scheme 1. Nanotube Functionalization Process

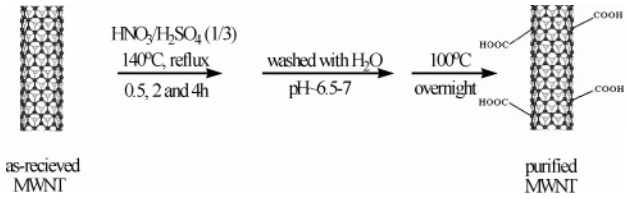

Scheme 2. Structure of PET−MWNT Nanocomposites

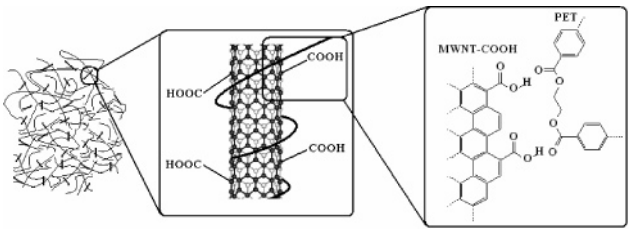

the tubes that leads to the formation of aggregations, which is a major issue in polymer nanocomposites.

Experimental Section

Materials. An Eastman PET 9921was used in the present study while the multiwall nanotubes (MW−NT) were purchased from Nanostructured & Amorphous Materials, NM (outside diameter 10−30 nm, length 1−10 μm and purity >80%).

Acidic Treatment. The as received nanotubes were treated with a HNO_3/H_2SO_4 (1/3) solution (40 mL/g NT) at 140 °C for 0.5, 2, and 4 h, yielding three samples named 05h, 2h, and 4h, respectively. Herewith, the tubes were washed with deionized water until the pH of the washings was around 7 (6.5−7). Finally, the nanotubes were dried in an oven at 100 °C under vacuum. This purification treatment which has been developed by Esumi et al.,[35] has been reported to introduce carbonyl groups onto the surface of the tubes (Scheme 1).

Melt Mixing. The PET pellets were premelted in a batch mixer at 280 °C for 2 min. Then the tubes were added (1.6% w/w) and the two ingredients were mixed for another 3 min under the same conditions yielding PET−MWNT nanocomposites (Scheme 2).

Film Preparation. The neat PET and PET−nanotube composite samples were melt-pressed at 3000 psig/280 °C and directly cooled on ice yielding transparent films of very low crystallinity named t, 05t, 2t, and 4t. Herewith, the samples were isothermally crystallized at 180 °C for 3 min yielding white samples named w, 05w, 2w, and 4w, respectively.

Measurements. Infrared transmission spectra were recorded using a Nicolet 850 FT-IR spectrometer equipped with an MCT/A detector as well as with a Nicolet Continuμm infrared microscope.

Table 1. Crystallinity, T_c. and fwhm Values of the Annealed PET and PET−MWNT Samples Measured during the First Run (both Heating and Cooling)

	first run, heating		first run, cooling	
	% crystallinity	%crystallinity	T_c (°C)	fwhm (°C)
PETw	22.9	29.8	192.58	14.89
PET05w	34.6	38.4	205.10	7.52
PET2w	36.7	38.9	208.24	6.89
PET4w	26.2	30.2	201.98	8.78

Each transmission measurement was the accumulation of 128 scans at 2 cm^{-1} spectral resolution. Curve fitting of the spectra was accomplished using the software package "Grams 32v5" (Galactic Industries Corp.). The peaks were simulated by a mixed Gaussian−Lorentzian function.

The Raman spectra were collected on the MicroRaman System HoloLab5000R with a Leica DMLP microscope (Kaiser Optical Inc.). The system was equipped with a NIR diode excitation laser at 785 nm and a CCD detector. Each measurement was the average of 250 accumulations of 1 s at 4 cm^{-1} spectral resolution. The laser power was 30 mW, the laser spot on the sample was 2 μm, and we used a microscope objective of 100×. The spectra were measured by the HoloGRAMS software and evaluated by the GRAMS/AI software V7 in the range from 3500 to 15 cm^{-1}.

A TA Instruments DSC Q 100 recorded the differential scanning calorimetry thermograms. The method selected involved the following: (i) the heating of the samples from 25 to 300 °C (first run: heating), (ii) the subsequent cooling to −10 °C (first run: cooling), and finally (iii) the heating to 300 °C (second run: heating); the heating rate in all cases was 10 °C/min. The percent crystallinity of the samples was calculated using the ratio of the ΔH_f values of the samples over the ΔH_f^0 of the perfect crystal (140 J/g).[36] In the case of the PET−MWNT samples, the crystallinity values were corrected considering the amount of the nanotubes added.

Results and Discussion

Introduction of COOH Groups onto the MWNT. Multiwall nanotubes that have undergone acidic treatment present the characteristic infrared peaks of carbonyl groups (Figure 1, parts a and b). The peak between 1354 and 1366 cm^{-1} is attributed to O−H deformation. The peak at 1717−1723 cm^{-1} is attributed to the C═O stretching mode of carboxylic acids[37] whereas the peaks at 3180 and 3329−3335 cm^{-1} are attributed to O−H stretching of carboxylic acid monomers and carboxylic acids with intermolecular hydrogen bonds, respectively. Because of carbon nanotubes texture (black powder) the quality of the spectra is not the desired, nevertheless the spectroscopic data presented make clear that COOH groups have been introduced

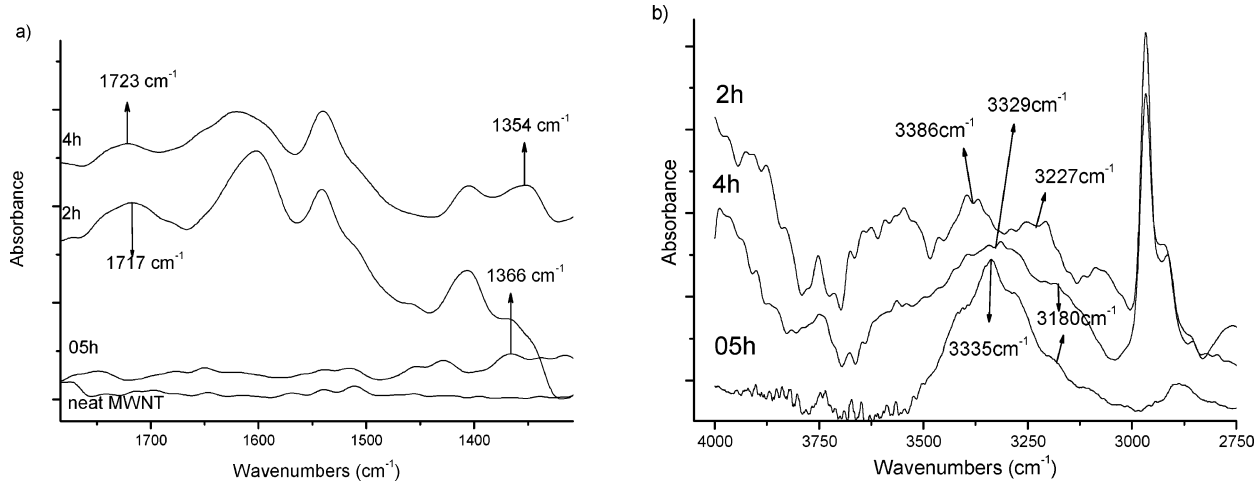

Figure 1. FTIR spectra of the acid-treated nanotubes (a) 1760−1300 and (b) 4050−2750 cm^{-1} spectral regions.

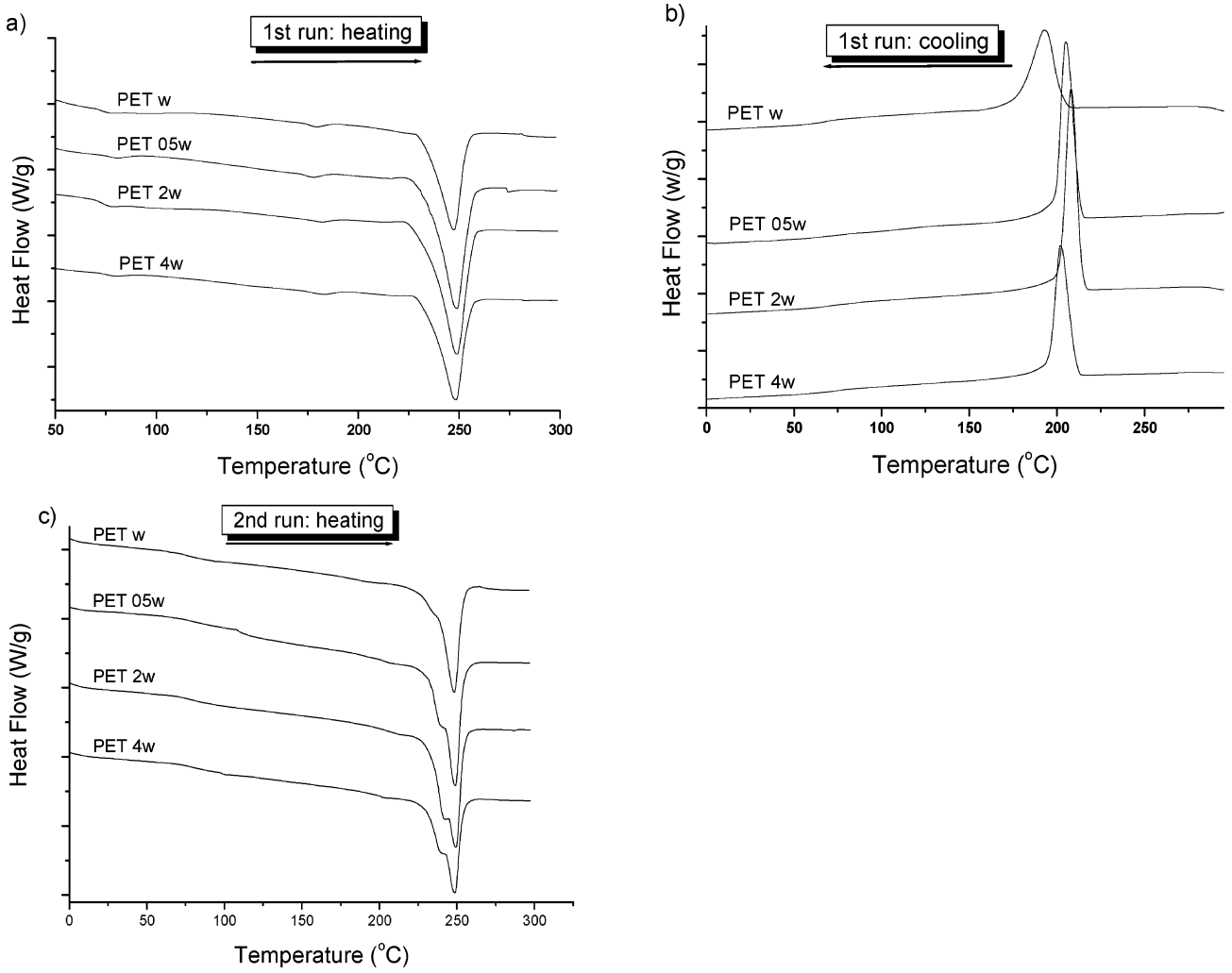

Figure 2. DSC thermograms of the annealed PET and PET−MWNT samples during the following runs: (a) first run, heating; (b) first run, cooling; (c) 2nd run, heating.

onto the nanotube surface. Thus, even if in the case of the 05h treated tubes the peak near 1720 cm^{-1} is absent (Figure 1a) the presence of COOH groups is manifested by the 3150−3350 cm^{-1} region (Figure 1b) while on the other hand even in the later region is clearly not safe to be used for the 2h sample it is fortunately demonstrated that this sample bears the 1717 and 1366 cm^{-1} peaks (Figure 1a). No C−C bond vibration was observed due to the fact that C−C bonds of the tubes are of high symmetry and therefore inactive in the infrared. As a matter of fact, this is the reason carbon nanotubes provide neat Raman spectra but poor infrared spectra or (in the case of untreated tubes) none at all.

Effect of MWNT—COOH on the Crystallization of PET. Differential scanning calorimetry (DSC) measurements were conducted on both annealed (white) and as molded (transparent) samples in an attempt to evaluate the effect that MWNT bear on the crystallization behavior of PET. The crystallinity of the 05w and 2w samples was found to be higher than that of neat PET, while the 4w sample showed no significant increase; similar results were observed for the crystallization of the samples during the cooling phase that followed (Table 1). Even though the presence of the nanotubes was not found to affect either the melting temperature (T_m) or the width of the melting peak (Figure 2a), this was not the case during the cooling of the samples. As shown in Figure 2b, the crystallization temperature (T_c) differs among the samples and so does the width of the crystallization peak. Table 1 shows that the T_c values increase and the full width at half-maximum (fwhm) of the crystallization peaks decreases as crystallinity rises. This observation leads to the conclusion that the presence of the nanotubes not only increases the crystallinity but also leads to a more perfect crystal formation.

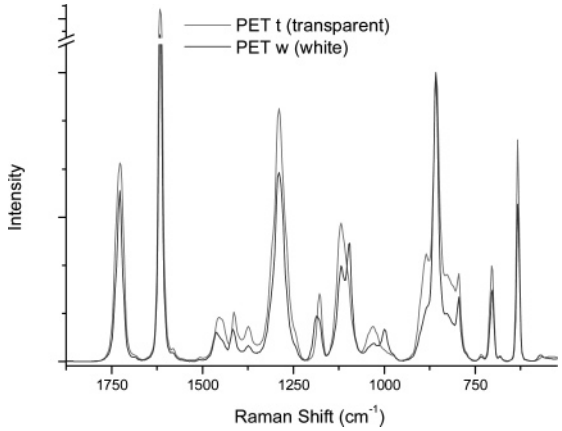

Figure 3. Raman spectra of pristine and annealed PET samples.

Finally, the second run heating demonstrated a double melt peak for all samples, which is least obvious in neat PET (Figure 2c). This effect was also apparent for the as-molded specimens (data not shown here due to curve similarity). The multiple melting peak behavior of semicrystalline polymers crystallized

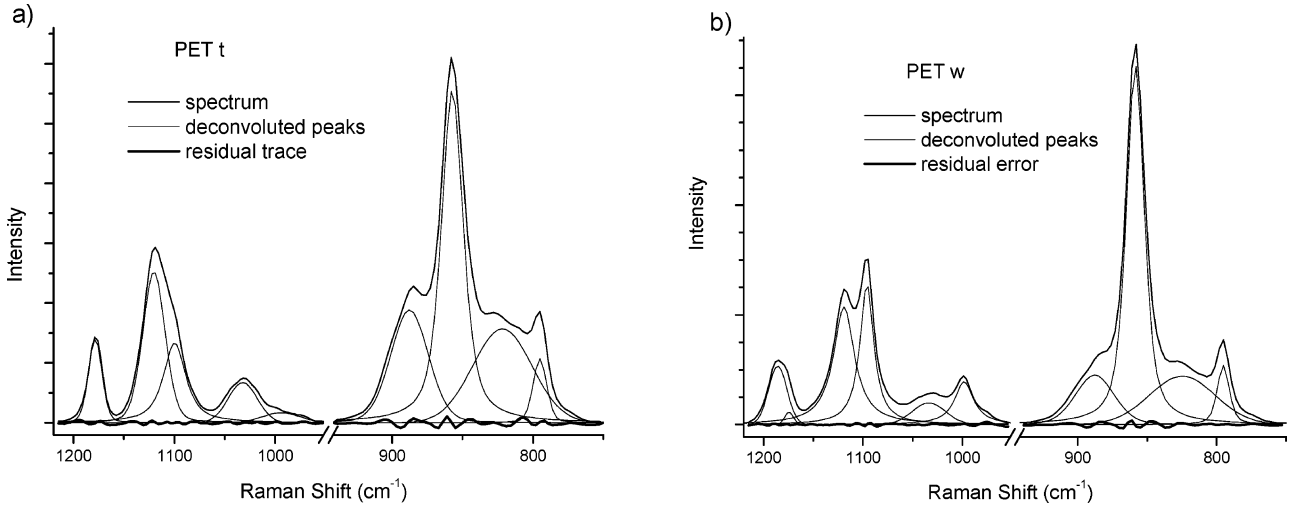

Figure 4. Deconvoluted spectrum of the (a) pristine and (b) annealed PET samples (1220−750 cm^{-1} spectral region).

from the melt has been investigated extensively and it is proposed to link to partial melting, re-crystallization, and remelting (mrr), to distribution of crystals with different lamellar thickness, and to melting of different crystal structures.[38] The annealing process led to a rapid formation of crystals which made this effect less obvious during the first run. In contrast, slow cooling treatment during the first run allows enough time for segregation of the different crystalline fractions to form two distinct morphologies resulting in the double peaks,[39] demonstrated during the second run heating. In the case of isothermally crystallized PET, it is suggested that the double melting behavior is associated with the mrr process.[40] Nevertheless, it is generally not possible to detect the recrystallization exotherm in the conventional DSC scan due to its superposition to the melting endotherm. In the examined case, neat PET demonstrates a narrow single peak accompanied by a negligible second peak while in the case of the PET nanocomposites there is a well-defined peak next to the main peak. Thus, it is concluded that the appearance of the mrr effect was strongly assisted by the presence of the nanotubes.

Effect of MWNT—COOH on the Conformations of PET Chains. Raman spectroscopy is a powerful tool when it comes to study chain conformations and crystallinity in macromolecular chains. PET has been widely studied via the use of Raman spectroscopy.[23,24,26,28,32,41−43] Figure 3 depicts the effect of the annealing process on the Raman spectrum of PET while Figure 4 shows the deconvoluted spectrum of the pristine and annealed PET samples (1220−750 cm^{-1} spectral region).

In the present study the peak at 1120 cm^{-1} (aromatic ring mode υ_1[44] or ring CH in plane bend or C−O stretch[25]) was used as a reference band since it is not affected by the thermal history and the crystallinity of the sample.[45,46] Figure 5 shows the reversed relative intensity of the 887 cm^{-1} band (CH_2 rocking mode of the gauche glycol moiety).[25,28,29,47]

The population of the gauche conformers appears to be higher in the w and 4w samples than in the 05w and 2w samples. The 887/1120 cm^{-1} peak ratio is plotted vs the noncrystalline fraction as calculated from the DSC measurements (Figure 6) to demonstrate the correlation between the two techniques. The PET−MWNT samples appear to follow a common linear pattern while neat PET appears to deviate from this pattern demonstrating higher amorphous fraction in respect to the gauche segments. Since the crystallinity values are solely defined by the trans crystalline segments, the 100 (% crystallinity by DSC) values represent an index of both the gauche and trans noncrystalline

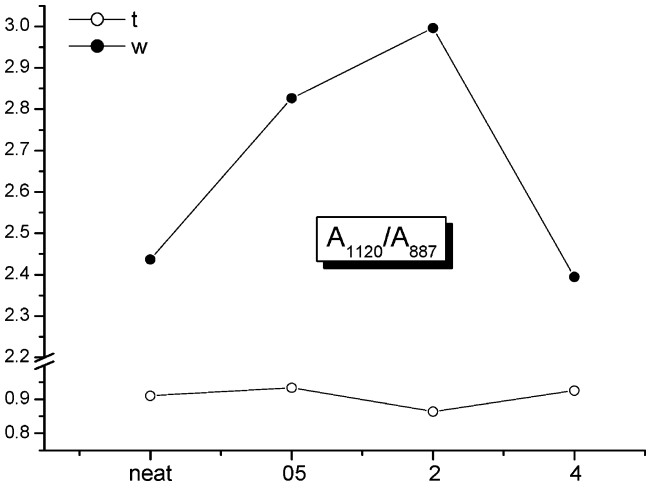

Figure 5. Reversed normalized intensity of the 887 cm^{-1} band of the annealed neat PET and PET−MWNT samples.

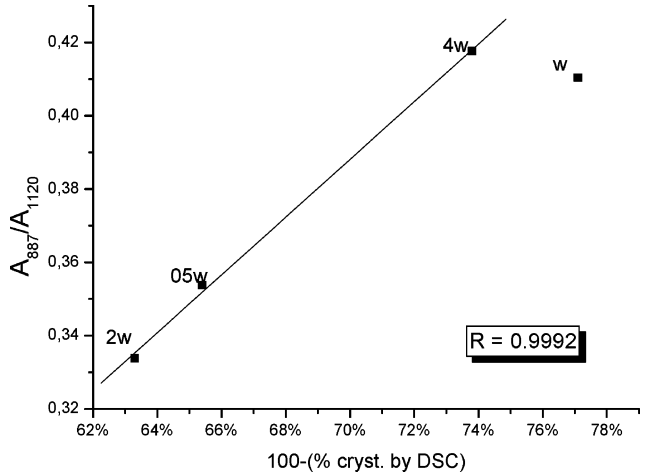

Figure 6. Normalized intensity of the 887 cm^{-1} band vs the noncrystalline fraction.

conformers. Thus, any deviation from a pattern correlating gauche conformers and DSC values may as well be translated as a variation of the trans noncrystalline conformers. Therefore, it can be concluded that more trans glycol conformers are in the noncrystalline phase of neat PET than in the PET−MWNT samples.

To study the effect of the nanotubes on the trans conformers of PET, the bands at 1100, 997, 857, and 1186 cm^{-1} were

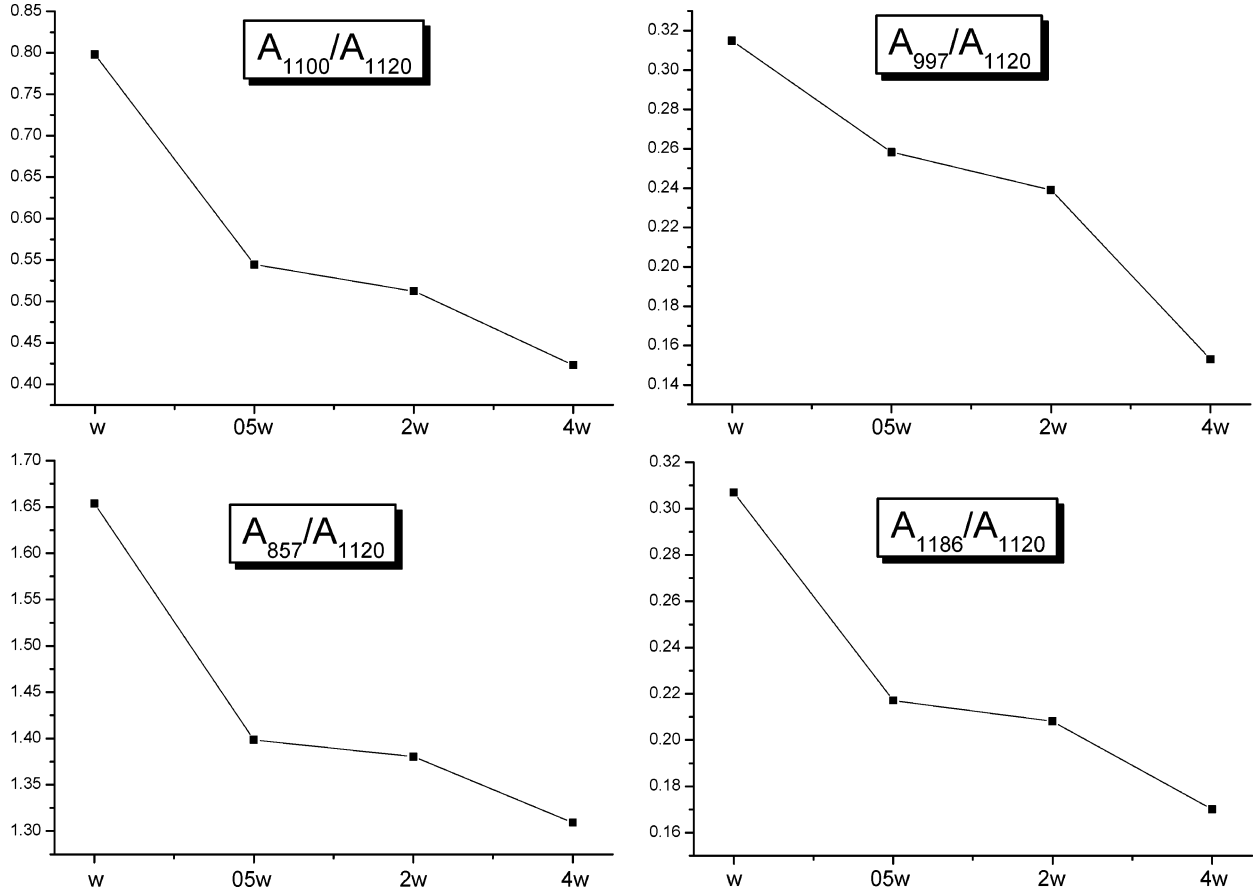

Figure 7. Normalized intensities of the 1100, 997, 857, and 1186 cm^{-1} bands of the annealed neat PET and PET−MWNT samples.

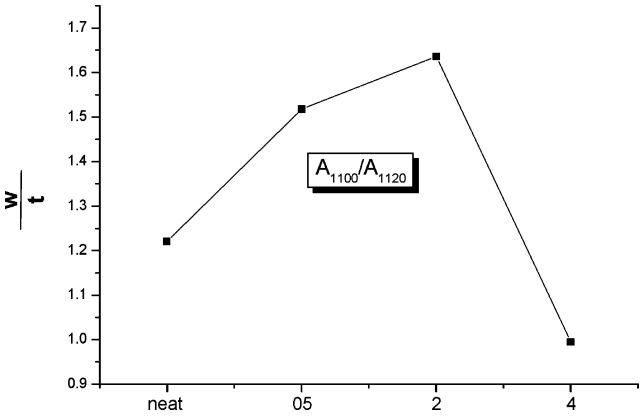

Figure 8. Ratio of the 1100 cm^{-1} band normalized intensities of the annealed (white) over the pristine (transparent) samples.

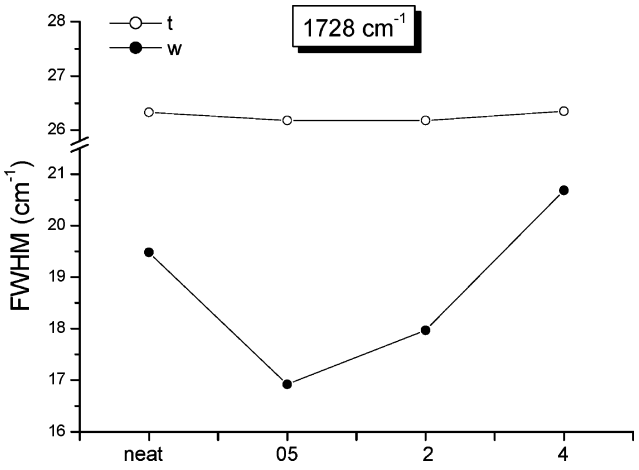

Figure 9. Full width at half-maximum (fwhm) values of the 1728 cm^{-1} band of the annealed neat PET and PET−MWNT samples.

normalized using the 1120 cm^{-1} band as in the case of the gauche conformers. The band at 1100 cm^{-1} (combination of ring C−C, ester *C*(*O*)-O and ethylene glycol C−C stretching modes[42]) is characteristic of the *all trans* (TtT_B) conformation[28] and has been widely used for the indirect estimation of crystallinity.[28,41,45,48] Nevertheless, there are many researchers that believe that this band is not a safe tool to predict crystallinity.[32,42] Likewise the bands at 997 cm^{-1} (either the symmetric stretching of the O−CH_2 bond[42,49] or the stretching of the C−C bond in ethylene glycol units[25,28,49,50]) and 1186 cm^{-1} (ring mode)[29,51] which appear after annealing, have also been associated with the crystalline phase of PET.[52] Finally, the band at 857 cm^{-1} (either the B_g ring CH out-of-plane bending mode or a complex A_g mode,[28] mainly involving ring C−C and *C*(*O*)−O stretches[42]) is reported to increase during annealing.[29,51]

Figure 7 shows that the neat PET sample has relatively more trans conformers than the 05w and 2w samples and even more than the 4w. The enriched population of trans conformers for the neat PET sample is due to the fact that the neat PET sample has a substantial quantity of trans conformers in the noncrystalline phase. Obviously the DSC crystallinity results which refer to trans-crystalline conformers and the gauche conformers population seem to contradict the later findings since they refer to two out of three conformations of PET. On the other hand the ratios in Figure 7 refer to a "mixture" of trans-crystalline and trans-noncrystalline conformations. Thus, the higher trans values observed for the neat PET sample strengths the conclusion that it has a significant amount of trans conformers in

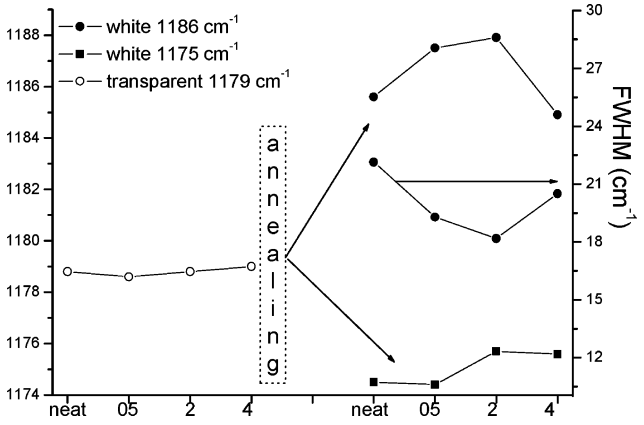

Figure 10. Split of the 1179 cm^{-1} peak due to the annealing process and full width at half-maximum (fwhm) values of the 1186 cm^{-1} band of the annealed neat PET and PET−MWNT samples.

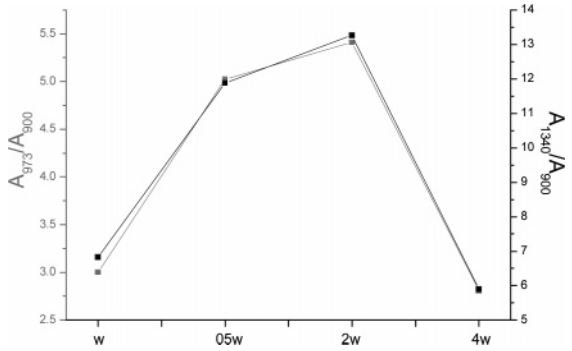

Figure 11. Normalized intensities of the 973 and 1340 cm^{-1} bands of the annealed neat PET and PET−MWNT samples.

noncrystalline regions adding up to the trans conformers population.

Figure 8 depicts the ratio of the 1100 cm^{-1} normalized peak of the w samples over the corresponding of the t samples. The 2w sample demonstrates the sharpest increase (ratio = 1.66) of the *all* trans sequences due to the annealing process, less intense was the transformation for the 05w and w samples (1.52 and 1.22 respectively) while the all trans sequences of the 4w sample seem to be least affected by the annealing process (0.99).

The width of the A_g C═O vibration at 1728 cm^{-1} has been associated with the sample's density and has been used indirectly as an index of crystallinity.[29,48,51] The fwhm values of this peak are depicted in Figure 9, where an increase in sample density is evident for all the annealed samples, especially the 05w and 2w which have also shown higher crystallinity (DSC measurements).

The peak at 1186 cm^{-1} which appears after the annealing process emerges from a split of the 1179 cm^{-1} peak as shown in Figure 10. Both the fwhm and the frequency shifts among the annealed samples appear to be affected by the crystallinity. Thus, the samples of higher crystallinity (2w and 05w) demonstrate sharper and more shifted bands in comparison to the 4w and w samples (Figure 10).

To describe the transformation that takes place among the polymeric chains during the annealing process, infrared bands representative of the various conformations of PET were also compared.

The ratios of the bands located at 1340 cm^{-1} (CH_2 wagging of the ethylene glycol segments trans)[53] and 973 cm^{-1} (antisymmetric C−O stretching trans −O−C−C−O− groups)[23,54−58] over the band at 900 cm^{-1} (CH_2 rocking gauche)[23,54,55,58,59] appear to follow the exact same pattern as shown by Raman data in Figure 5 (Figure 11).

The *trans*/*gauche* ratio in both cases is higher for the samples of higher crystallinity (05w and 2w). Crystallinity measured via DSC appears to be a linear function of the ratios only in the case of the nanocomposite samples and not in the case of neat PET exactly as in the Raman measurements. In detail, the neat PET sample's crystallinity should be higher judging from its *trans/gauche* ratio. Nevertheless, this is not the case proving once again that neat PET bears much more trans conformers in noncrystalline regions (Figure 12a). Noteworthy is the fact that both Raman and FT-IR not only lead to the same conclusions but also perfectly match each other as shown in Figure 12b.

Conclusions

FT-IR spectroscopic measurements verified the introduction of COOH groups onto the surface of the multiwall-nanotubes via the acidic treatment process. The PET- 05w and 2w samples demonstrated higher values of crystallinity (first run: heating and cooling) than neat PET, while the 4w sample showed no significant increase. The presence of the nanotubes not only increased crystallinity but also led to a more perfect crystal formation since T_c increased and fwhm of the crystallization peak decreased as crystallinity increased. The second run revealed that MWNT−COOH strongly induce the melting−recrystallizing−remelting (mrr) effect yielding a double melting peak. Raman spectroscopic measurements showed that the population of the gauche conformers was higher in the w and

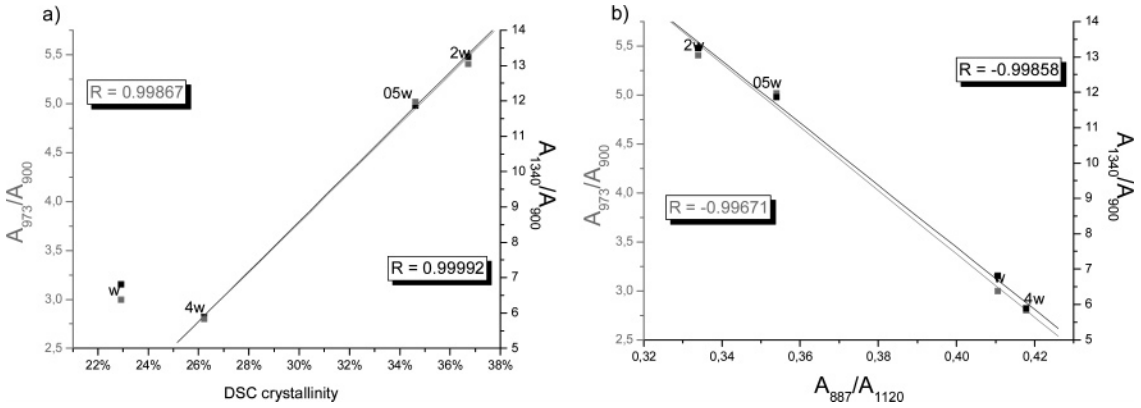

Figure 12. Normalized intensities of the 973 and 1340 cm^{-1} bands vs (a) the % crystallinity and (b) the normalized intensity of the 887 cm^{-1} (Raman) band.

4w samples than in the 05w and 2w. Correlation between Raman and DSC measurements showed that neat PET has relatively more trans conformers in the noncrystalline phase than the PET−MWNT samples. The DSC measurements were consistent with the fwhm of the 1728 and 1186 cm^{-1} peaks which are commonly used to estimate crystallinity. FT-IR measurements were also in agreement with the abovementioned conclusions and in complete agreement with the Raman findings. In particular, FT-IR spectroscopy also showed that the trans/gauche ratio was higher for the samples of higher crystallinity (05w and 2w). Finally, as in the case of the Raman/DSC correlation, FT-IR measurements showed that the neat PET bears much more trans conformers in noncrystalline regions in comparison to the PET−MWNT samples. The authors based on their findings support that the addition of functionalized nanotubes increases the crystallinity by incorporating trans conformers, which originally would be in noncrystalline regions (in neat PET), into the crystalline phase, on top of that the crystals formed seem to be of higher order having a narrower size distribution.

Acknowledgment. We are grateful to Professor J. Karger-Kocsis and Dr. K. G. Gatos of the "Institut für Verbundwerkstoffe GmbH, Universität Kaiserslautern", Kaiserslautern, Germany, for supplying the poly(ethylene terephthalate) samples used in the present study. This work was financially supported by the Greek Ministry of Development under the research grant PENED 2001-136, as well as by the European Network of Excellence, NanoFun-Poly, No FP6-500361-2, Sixth Framework Program.

References and Notes

(1) Hu, G.; Zhao, C.; Zhang, S.; Yang, M.; Wang, Z. *Polymer* **2006**, *47*, 480−488.
(2) Iijima, S. *Nature* **1991**, *354*, 56−58.
(3) Bin, Y.; Kitanaka, M.; Zhu, D.; Matsuo, M. *Macromolecules* **2003**, *36*, 6213−6219.
(4) De Heer, W. A.; Chatelain, A.; Ugarte, D. *Science* **1995**, *270*, 1179−1180.
(5) Choi, W. B.; Chumg, D. S.; Kang, J. H.; Kim, H. Y.; Jin, Y. W.; Han, I. T.; Lee, Y. H.; Jung, J. E.; Lee, N. S.; Park, G. S.; Kim, J. M. *Appl. Phys. Lett.* **1999**, *75*, 3129−3131.
(6) Fan, S.; Chapline, M. G.; Franklin, N. R.; Tombler, T. W.; Cassell, A. M.; Dai, H. *Science* **1999**, *283*, 512−514.
(7) Martel, R.; Schmidt, T.; Shea, H. R.; Hertel, T.; Avouris, Ph. *Appl. Phys. Lett.* **1998**, *73*, 2447−2249.
(8) Dai, H.; Hafner, J. H.; Rinzler, A. G.; Colbert, D. T.; Smalley, R. E. *Nature* **1996**, *384*, 147−151.
(9) Wong, S. S.; Joselevich, E.; Woolley, A. T.; Cheung, C. L.; Lieber, C. M. *Nature* **1998**, *394*, 52−55.
(10) Ishihara, T.; Kawahara, A.; Nishiguchi, H.; Yoshio, M.; Takita, Y. *J. Power Sources* **2001**, *97*−*98*, 129−132.
(11) Liu, C.; Fan, Y. Y.; Liu, M.; Cong, H. T.; Cheng, H. M.; Dresselhaus, M. S. *Science* **1999**, *1286*, 1127−1129.
(12) Rajalakshmi, N.; Dhathathreyan, K. S.; Govindaraj, A.; Satishkumar, B. C. *Electrochim. Acta* **2000**, *45*, 4511−4515.
(13) Fuhrer, M. S. *IEEE Trans. Nanotechnol.* **2002**, *1*, 78.
(14) Tans, S. J.; Verschueren, A. R. M.; Dekker: C. *Nature* **1998**, *393*, 49−51.
(15) Kim, P.; Lieber, C. M. *Science* **1999**, *286*, 2148−2150.
(16) Kong, J.; Franklin, N.; Zhou, C.; Peng, S.; Cho, J. J.; Dai, H. *Science* **2000**, *287*, 622−625.
(17) Wu, M.; Shaw, L. L. *Int. J. Hydrogen Energy* **2005**, *30*, 373−380.
(18) Wu, M.; Shaw, L. L. *J. Power Sources* **2004**, *136*, 37−44.
(19) Parikh, K.; Cattanach, K.; Rao, R.; Suh, D. S.; Wu, A.; Manohar, S. K. *Sens. Actuators B* **2006**, *113*, 55−63.
(20) Li, Z.; Luo, G.; Wei, F.; Huang, Y. *Comput. Sci. Technol.* **2006**, *66*, 1022−1029.
(21) Lee, H. J.; Oh, S. J.; Choi, J. Y.; Kim, J. W.; Han, J.; Tan, L. S.; Baek, J. B. *Chem. Mater.* **2005**, *17*, 5057−5064.
(22) Shin, D. H.; Yoon, K. H.; Kwon, O. H.; Min, B. G.; Hwang, C. I. *J. Appl. Polym. Sci.* **2006**, *99*, 900−904.
(23) Miyake, A. *J. Polym. Sci.* **1959**, *38*, 479−495.
(24) Manley, T. R.; Williams, D. A. *Polymer* **1969**, *10*, 339−384.
(25) Ward, I. M.; Wilding, M. A. *Polymer* **1977**, *18*, 327−335.
(26) Daubeny, R.; Bunn, C. W.; Brown, C. J. *Proc. R. Soc.* **1954**, *A226*, 531−542.
(27) D'Esposito, L.; Koenig, J. L. *J. Polym. Sci., Polym. Phys. Ed.* **1976**, *14*, 1731−1741.
(28) Štokr, J.; Schneider, B.; Doskoèilová, D.; Lobby, J.; Sedláček, P. *Polymer* 1982, *23*, 714−721.
(29) Rodríguez-Cabello, J. C.; Quintanilla, L.; Pastor, J. M. *J. Raman Spectrosc.* **1994**, *25*, 335−344.
(30) Lu, X. F.; Hay, J. N. *Polymer* **2001**, *42*, 8055−8067.
(31) Lin, S. B.; Koenig, J. L. *J. Polym. Sci., Polym. Phys. Ed.* **1982**, *20*, 2277−2295.
(32) Adar, F.; Noether, H. *Polymer* **1985**, *26*, 1935−1943.
(33) Dargent, E.; Grenet, J.; Auvray, X. *J. Therm. Anal.* **1994**, *41*, 1409−1415.
(34) Ajji, A.; Guévremont, J.; Cole, K. C.; Dumoulin, M. M. *Polymer* **1996**, *37*, 3707−3714.
(35) Esumi, K.; Ishigami, A.; Nakajima, A.; Sawada, K.; Honda, H. *Carbon* **1996**, *34*, 279−281.
(36) Mehta, A.; Gaur, H.; Wunderlich, B. *J. Polym. Sci., Polym. Phys. Ed.* **1978**, *16*, 289−296.
(37) Chen, J.; Hamon, M. A.; Hu, H.; Chen, Y.; Rao, A. M.; Eklund, P. C.; Haddon, R. C. *Science* **1998**, *282*, 95−98.
(38) Cser, F.; Rasoul, F.; Kosior, E. *J. Therm. Anal. Cal.* **1997**, *50*, 727−744.
(39) Awaja, F.; Daver, F.; Kosior, E.; Cser, F. *J. Therm. Anal. Cal.* **2004**, *78*, 865−884.
(40) Medellin-Rodriguez, F. J.; Phillips, P. J.; Lin, J. S.; Campos, R. *J. Polym. Sci., Part B: Polym. Phys.* **1997**, *35*, 1757−1774.
(41) Melveger, A. *J. Polym. Sci. (A-2)* **1972**, *10*, 317−322.
(42) Boerio, F. J.; Bahl, S. K.; McGraw, G. E. *J. Polym. Sci., Polym. Phys. Ed.* **1976**, *14*, 1029−1046.
(43) Kandilioti, G.; Govaris, G.; Gregoriou, V. G. *Appl. Spectrosc.* **2004**, *58*, 1082−1092.
(44) Derault, J.; Gall, M. J.; Hendra, P. J.; Ellis, V.; Cudby, M. E. A.; Willis, H. A. *Proc. 2nd Eur. Symp. Polym. Spectrosc.* **1975**, *85*.
(45) Bulkin, B. J.; Lewin, M.; DeBlase, F. J. *Macromolecules* **1985**, *18*, 2587−2594.
(46) Pastor, J. M.; Gonzalez, A.; De Saja, J. A. *J. Appl. Polym. Sci.* **1989**, *38*, 2283−2288.
(47) Yang, X.; Long, F.; Shen, D.; Qian, R. *Polym. Commun.* **1991**, *32*, 125−128.
(48) Kazarian, S. G.; Brantley, N. H.; Eckert, C. A. *Vibr. Spectrosc.* **1999**, *19*, 277−283.
(49) Yang, S.; Michielsen, S. *Macromolecules* **2002**, *35*, 10108−10113.
(50) Everall, N.; Tayler, P.; Chalmers, J. M.; MacKerron, D.; Ferwerda, R.; Van der Maas, J. H. *Polymer* **1994**, *35*, 3184−3192.
(51) Quintanilla, L.; Rodríguez-Cabello, J. C.; Pastor, J. M. *J. Raman Spectrosc.* **1994**, *25*, 345−351.
(52) Fleming, O. S.; Kazarian, S. G.; Bach, E.; Schollmeyer, E. *Polymer* **2005**, *46*, 2943−2949.
(53) Pearce, R.; Cole, K. C.; Ajji, A.; Dumoulin, M. M. *Polym. Eng. Sci.* **1997**, *37*, 1795−1800.
(54) Cole, K. C.; Ajji, A.; Pellerin, E. *Macromol. Symp.* **2002**, *184*, 1−18.
(55) Kitano, Y.; Kinoshita, Y.; Ashida, T. *Polymer* **1995**, *36*, 1947−1955.
(56) Cobbs, W. H. Jr; Burton, R. L. *J. Polym. Sci.* **1953**, *10*, 275.
(57) Hannon, M. J.; Koenig, J. L. *J. Polym. Sci. (A-2)* **1969**, *7*, 1085−1099.
(58) Aharoni, S. M.; Sharma, R. K.; Szobota, J. S.; Vernick, D. A. *J. Appl. Polym. Sci.* **1983**, *28*, 2177−2186.
(59) Miller, R. G.; Willis, H. A. *J. Polym. Sci.* **1956**, *19*, 485−494.

MA0613584